JOURNAL OF Applied Polymer SCIENCE

Synthesis of Fluoroalkyl-Modified Polyester and Its Application in Improving the Hydrophobicity and Oleophobicity of Cured Polyester Coatings

Jinsu Xiong, Lei Xia, Baoqing Shentu, Zhixue Weng

State Key Lab of Chemical Engineering, Department of Chemical and Biological Engineering, Zhejiang University, Hangzhou 310027, China

Correspondence to: B. Shentu (E-mail; shentu@zju.edu.cn).

ABSTRACT: The fluoroalkyl-modified polyester (PE-F_n) was synthesized by the reaction of polyester resin (PE) and fluorinated isocyanate, and the structure of the synthesized product was characterized by proton nuclear magnetic resonance (^{1}H-NMR) and fluorine nuclear magnetic resonance (^{19}F-NMR). The water and oil wettability of the cured PE coatings with PE-F_n as additives was investigated by contact angle meter. The results showed that the introduction of an extremely low concentration of PE-F_n into PE led to the increase in contact angle of water and diiodomethane on cured PE coatings, and the decrease in the surface free energy. The X-ray photoelectron spectroscopic (XPS) analysis showed that the F/C molar ratio in the outer few nanometers was significantly higher than that in the bulk, indicating that the fluoroalkyl groups in PE-F_n had enriched on the coating surface. It was also found that longer fluoroalkyl groups and fluoroalkyl groups with —CF_3 at its end had the higher tendency to aggregate on the coating surface. The topological structures of the cured coatings were recorded by an atomic force microscope under tapping mode and the results revealed that there was a strong surface segregation of fluorinated species. © 2013 Wiley Periodicals, Inc. J. Appl. Polym. Sci. **2014**, *131*, 39812.

INTRODUCTION

Powder coating have many desirable advantages, for example, high mechanical strength, convenient transport and storage, environmental compliance, and good adhesion to a variety of substrates.[1] These advantages afforded by powder coating have led to a rapid growth in their use in different fields, such as machinery, construction, transportations, electrical, and electronic devices.[2] However, the cured coating of common powder coating is often affected by moisture and water-soluble corrosion agents in outdoor environment, which results in the decline of the durability and service life of the cured coating.[3] Moreover, the oil and organic solvent is also unfavorable to the performance of the cured coatings when applied to some cases like pipes, range hoods, and automobile engine.[4] Thus, it is important to improve the hydrophobicity and oleophobicity of the powder coating. The fluorinated coatings have received much attention in recent years because of their unique performances provided by the fluorine atoms, such as thermal stability, good weather ability, solvent resistance, and excellent water/oil repellency.[5,6] Therefore, the introduction of fluorine into common powder coating could be a good solution to solve the aforementioned problems.

There have been reports about the preparation of various kinds of fluorinated powder coatings. Plich–Pitera synthesized blocked polyisocyanates containing fluorine atoms as crosslinking agents for powder coating, and thus introduced the fluorine into the powder coating.[7] In our previous study, we have synthesized fluorine-containing polyester (PE) and obtained cured coatings with water and oil repellence.[8] However, according to our previous study, the contact angle of water and diiodomethane can reach only 108° and 69°, respectively at the fluorine content of 2.43% and the amount of fluorine-containing monomers used in the reaction is high. Thus, it is essential to reduce the fluorine content and increase the utilization of fluorine in order to improve the hydrophobicity and oleophobicity of powder coating. Moreover, the enrichment degree of fluoroalkyl groups on the coating surface also needs to be further improved.

To solve the aforementioned problems, it is expected to improve the hydrophobicity and oleophobicity of the coating surface through the introduction of a small amount of fluorinated additives into the formulations. The fluorinated additives, exhibiting lower surface tension as compared to other components in the organic coatings, have the higher tendency to migrate towards the air/coating interface, which strongly affects

Table I. Structure of PE and PE-F$_n$

Sample	Structure
PE	
PE-F$_{12}$	
PE-F$_{13}$	
PE-F$_{17}$	

the hydrophobic and oleophobic properties of the coatings.[9] It is, therefore, only a very small quantity of fluorinated additives is needed to improve the hydrophobicity and oleophobicity of the coating surface. However, researches about fluorinated polymers used as additives in organic coatings mainly concentrated on liquid coatings containing solvents,[10,11] which is not environmental friendly, and there is few reports about the preparation of fluoroalkyl-modified PE used as additives in powder coatings. Thus, it is essential to synthesis the fluorinated additives applied in powder coating with the aim to prepare hydrophobic and oleophobic cured coatings.

In this study, a series of PE-F$_n$ with different fluoroalkyl groups at its ends was synthesized by modifying the PE resin with fluorinated isocyanate. The structure of PE-F$_n$ was characterized by ^{1}H-NMR and ^{19}F-NMR. Fluorine content in PE-F$_n$ was determined by oxygen-flask combustion and fluoride selective electrode.[12] Water and oil wettability of cured coatings with PE-F$_n$ as additives was investigated by contact angle meter. The fluorine enrichment on the coating surface was examined by X-ray photoelectron spectroscopy (XPS). The topological structure of the cured coatings was examined by atomic force microscopy (AFM) under tapping mode.

EXPERIMENTAL

Materials

1H,1H,7H-dodecafluoro-1-heptanol (DFHO) was purchased from Aladdin. 1H,1H,2H,2H- tetrahydroperfluoro-1-octanol and 1H,1H,2H,2H-tetrahydroperfluoro-1-decanol were supplied by Alfa Aesar. Tolylene-2,4-diisocyanate (TDI) was obtained from Sigma-Aldrich. Dibutyltin dilaurate (DBTDL) were purchased from Aladdin. 1,4-Butanediol (BDO), analytical reagent (AR), was supplied by Shanghai Crystal Pure Reagent. Phthalic anhydride (PA) and Epichlorohydrin (ECH) and acetic anhydride (AA), AR, were obtained from Shanghai Lingfeng Chemical Reagent. Tetraethylammonium bromide (TEAB) and N,N-dimethylfomamide (DMF), AR, were supplied by Sichuan West Reagent. Tetrahydrofuran (THF) and n-hexane, AR, were

purchased from Hangzhou Reagent. Calcium hydride, chemical reagent (CR), were obtained from National Pharmaceutical Group Chemical Reagent. Triglycidyl isocyanurate (TGIC, curing agent) and CaCO$_3$ were obtained from Deqing Brilliant Chemical. BYK-361N (flatting agent), BYK-364P (antifoaming agent) and BYK-220S (wetting agent) were obtained from Shanghai BYK solutions. BDO was dried with anhydrous 4 Å zeolite for 24 h and then vacuum-distilled. PA was recrystallized in acetic anhydride and then dried in vacuum oven at 70°C for 12 h. ECH was refluxed with calcium hydride at 145°C for 5 h and then distilled. TEAB was dried in vacuum oven at 70°C for 12 h. DMF was dried with calcium hydride for 24 h and then vacuum-distilled. Other reagents were used as received without further purification, unless otherwise stated.

Preparation of Polyester

An hydroxyl terminated PE was synthesized according to our former Ref. 13. 0.36 g (4.0×10^{-3} mol) of BDO, 16.3 g (1.1×10^{-1} mol) of PA, 0.21 g (1.0×10^{-3} mol) of TEAB, 9.25 g (1.0×10^{-1} mol) of ECH and 4 mL of DMF were charged into a dried 250 mL three-necked round-bottom flask equipped with a mechanical stirrer, condenser, and nitrogen inlet and outlet. The mixture was heated to 100°C and reacted for 1 h under nitrogen. Then the mixture was diluted with acetone and precipitated with water. The collected solid was dried in vacuum oven (1.3×10^3 Pa) at 100°C for 10 h. The hydroxyl value of PE was determined to be 15.3 mgNaOH/g by titration.[14] The number average molecular weight of PE was 5229 g/mol calculated from hydroxyl value.[15] The structure of PE was shown in Table I.

Preparation of Fluoroalkyl-Modified Polyester (PE-F$_n$)

The schematic outline for the reaction procedure was shown in Scheme 1. For the synthesis of PE-F$_{12}$, TDI (0.87 g/0.005 mol) diluted by THF (20 mL) was charged into a dried 250 mL four-necked round-bottom flask equipped with a mechanical stirrer, addition funnel, reflex condenser, and nitrogen inlet and outlet. After dissolving 0.1 wt % DBTDL, a solution of DFHO (1.69 g/0.0051 mol) predissolved with THF (20 mL) was added dropwise through the addition funnel. The reaction was maintained at 50°C for 2 h. In the second step, PE (6.53 g/0.0012 mol) and THF (20 mL) were added into a dried 250 mL four-necked round-bottom flask equipped with a mechanical stirrer, addition funnel, reflex condenser, and nitrogen inlet and outlet. After the flask was heated to 70°C, the product obtained from the first step was added dropwise through the addition funnel. The reaction was maintained at 70°C for 4 h. Then the mixture was poured into a large amount of n-hexane and the product was precipitated and collected by filtration. The collected solid was dried in vacuum oven (1.3×10^3 Pa) at 50°C for 24 h and then the product (PE-F$_{12}$), as a white powder was obtained with a yield of 91%.

With different fluoroalkyl alcohols (F$_n$-OH), PE-F$_{13}$ and PE-F$_{17}$ were obtained respectively by using the similar synthesis procedure. The yield of PE-F$_{13}$ and PE-F$_{17}$ were 89% and 85%, respectively.

### Preparation of Fluorinated Polyester Powder Coating

The PE-F$_n$ were mixed with PE as well as CaCO$_3$ (30 wt %), the curing agent (TGIC, 6 wt %), the flatting agent (BYK-361N,
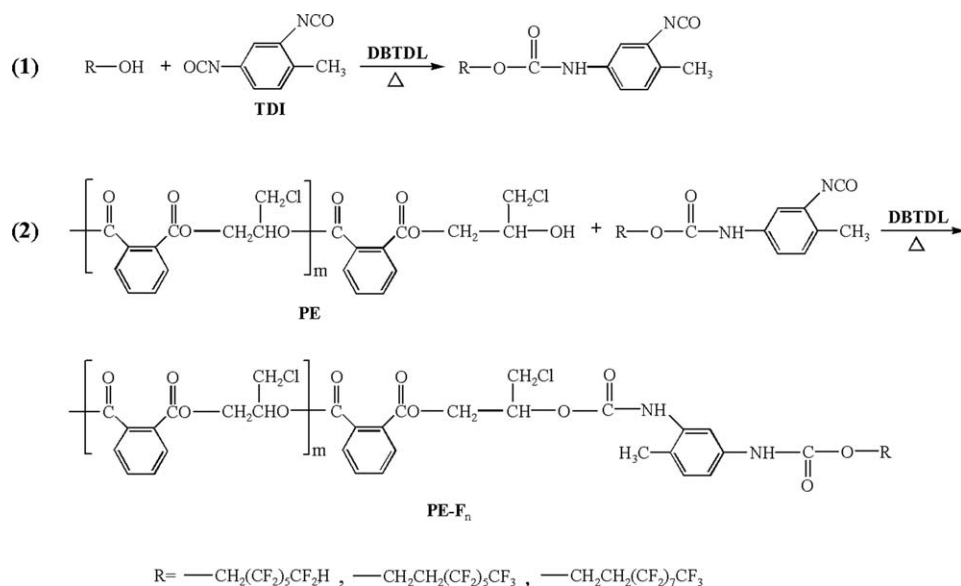
Scheme 1. Synthesis of PE-F$_n$.

1.5 wt %), the wetting agent (BYK-220S, 1.5 wt %), and the anti-foaming agent (BYK-364P, 1.5 wt %). The mixture was blended in a banbury mixer at 100°C for 10 min and the rotor speed of banbury was 80 rotor/min. Then, the mixture was pulverized to the average particle size of 80 μm. In addition, the concentration of PE-F$_n$ was varied from 0.25 to 2% in order to obtain different fluorine content in the PE powder coating (Table III).

Spraying and Curing of Fluorinated Polyester Powder Coating

The static spraying gun set at 60 kV was used to spray the coating powders onto the stainless steel plate. The $100 \times 50 \times 0.5$ mm^3 stainless steel plate was treated by degreasing and decontamination before used. The coated plates were cured at 180°C for 20 min and then cooled to room temperature.
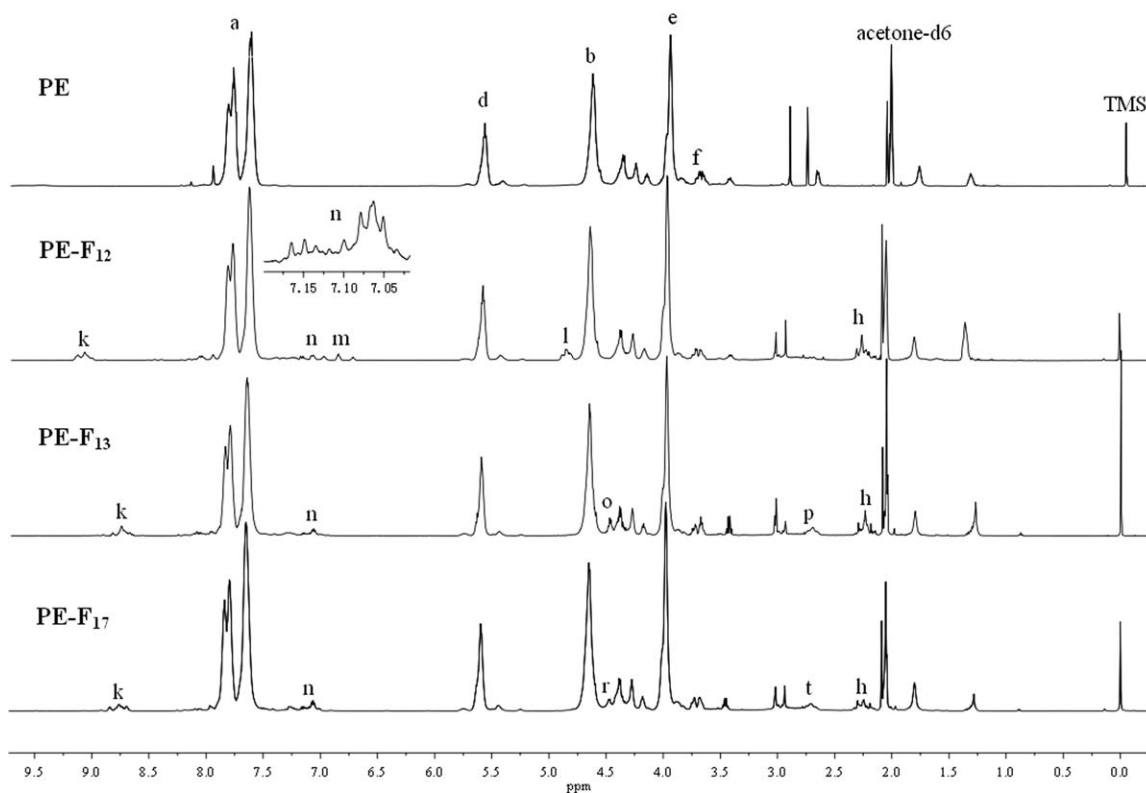
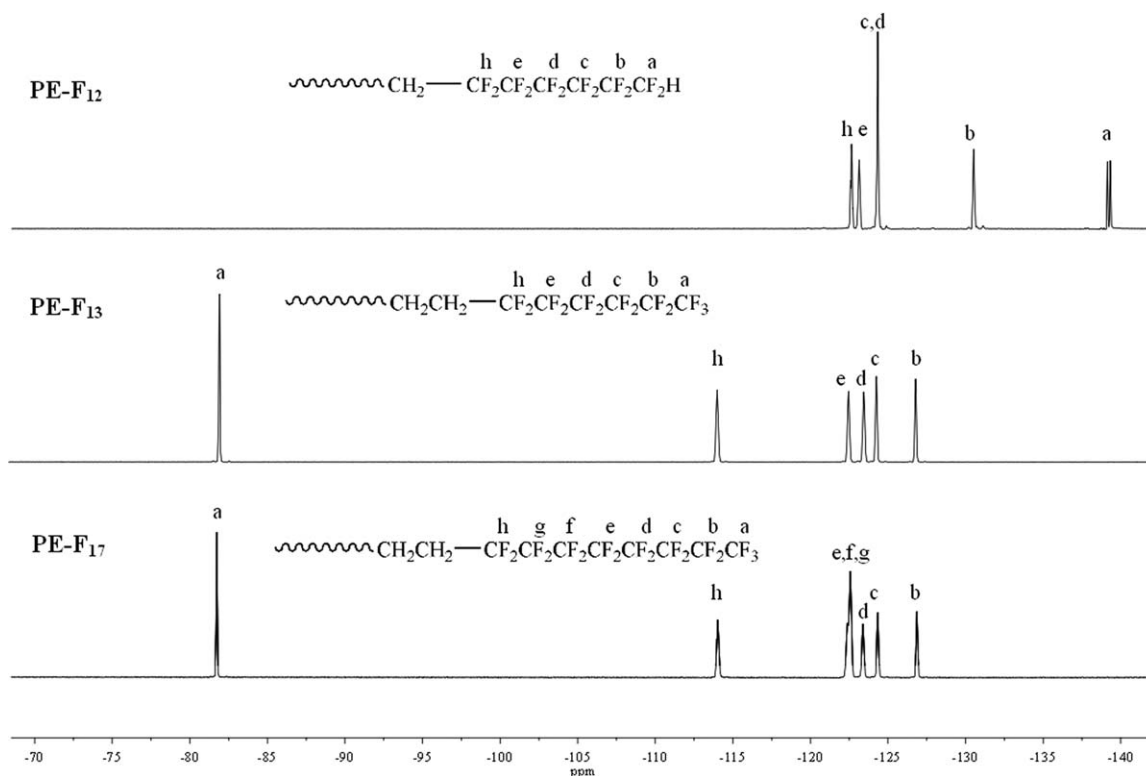**Figure 1.** ^{1}H-NMR spectra of PE and PE-F$_n$.

Figure 2. ^{19}F-NMR spectra of PE and PE-F$_n$.

Characterization

^{1}H-NMR and ^{19}F-NMR spectra were recorded with a Bruker AVANCE II nuclear magnetic resonance spectrometer using acetone-d$_6$ as solvent. The resolutions of ^{1}H-NMR and ^{19}F-NMR were 300 and 282 MHz, respectively.

The oxygen-flask combustion and fluoride selective electrode method was used to determine the fluorine content in PE-F$_n$.[12] The solution with the known fluorine ion concentration (from 0.005 to 100 mg/L) was prepared and measured with fluoride selective electrode. Thus, the relationship between potential and fluorine ion concentration was obtained. PE-F$_n$ was burnt completely under oxygen atmosphere in oxygen-flask and absorbed by NaOH solution. The solution was then measured with fluoride selective electrode and fluorine content in PE-F$_n$ was obtained according to the measured potential.

Contact angle measurement was performed with an OCA-20 contact angle meter equipped with a videocamera. Analysis was made at room temperature by means of the sessile drop technique. The measuring liquid was ion-exchanged water and diiodomethane. Three measurements were performed on every sample and the averaged value was used as the final result.

XPS spectra were collected on the VG ESCALAB MARK II X-ray photoelectron spectroscopy equipped with a MgKα X-ray source (hγ = 1253.6 eV). Spectra were acquired at three different takeoff angles: 15°, 45°, and 90°.[16] The pressure in the instrumental chamber was 1×10^{-8} mmHg. All the spectra were recorded at 0–1060 eV with a step internal of 0.5 eV. Survey and high resolution spectra (F$_{1s}$ and C$_{1s}$) were also recorded

for each sample with a step internal of 0.2 eV to determine the F/C molar ratio on the coating surface.

AFM images (both height and phase) were recorded under tapping mode on a Veeco Multimode SPM Nanoscope III instrument in air.

RESULTS AND DISCUSSION

Preparation and Structure of PE-F$_n$

PE-F$_n$ was prepared by the reaction of hydroxyl terminated PE, TDI, and fluoroalkyl alcohols (F$_n$-OH) using DBTDL as a catalyst (Scheme 1). TDI was the diisocyanate that contained primary and secondary isocyanate groups. The selectivity of the reaction between the alcohol and the primary isocyanate group was as high as 98% when tin used as the catalyst at low temperature.[17] Therefore, by controlling the F$_n$-OH/NCO molar ratio at 1 : 2, the fluoroalkyl group could be selectively grafted onto TDI, leaving the other isocyanate group for further reaction with the hydroxyl groups at the terminal of PE. By changing the species of fluoroalkyl alcohols in the reaction, three samples (PE-F$_{12}$, PE-F$_{13}$, and PE-F$_{17}$) were obtained with different fluoroalkyl groups at its ends. The molecular structure of PE and PE-F$_n$ was shown in Table I.

The ^{1}H-NMR spectra of original PE and PE-F$_n$ were shown in Figure 1. The ^{1}H-NMR spectrum of PE showed that the peaks at 7.5–8.0 ppm were assigned to the hydrogen atoms of substituted benzene (a). The peaks at 5.5–5.6 ppm were assigned to the hydrogen atoms of —CHO— (d). The peak at 4.5–4.7 ppm was ascribed to the hydrogen atoms of methylene (b). The

Table II. Fluorine Content of PE-F_n

Sample	Theoretical fluorine content (wt %)	Measured fluorine content (wt %)	Degree of modification (%)
PE-F_{12}	7.32	6.42 ± 0.06	87.70 ± 0.008
PE-F_{13}	7.84	6.92 ± 0.09	88.27 ± 0.011
PE-F_{17}	9.92	8.71 ± 0.07	87.80 ± 0.007

proton peak for —CH_2Cl (e) was found at 3.8–4.0 ppm. The peaks at 3.65–3.72 ppm were assigned to the hydrogen atoms of methane (f) connected to —OH.

The ^{1}H-NMR spectra of PE-F_n showed that its characteristic peaks of backbone were coincided with that of original PE and some new peaks were present. For instance, in the ^{1}H-NMR spectrum of PE-F_{12}, the new peaks at 7.02–7.20 ppm were assigned to the hydrogen atoms of substituted benzene (n). The peaks of methine proton of —CF_2H (m) and methylene protons of —CH_2—CF_2— (l) were observed at 6.5–7.15 ppm and 4.78–4.95 ppm, respectively, which proved the presence of fluoroalkyl groups. The new proton peaks for —NH—C(O) — (k) were found at 8.99–9.22 ppm. The peaks at 2.11–2.38 ppm were assigned to the hydrogen atoms of methyl (h) connected to benzene ring. The degree of modification was 88.3%, which could be estimated from the integral values of peaks at 4.78–4.95 ppm (the methylene protons of —CH_2— connected to —CF_2—) and 3.8–4.0 ppm (the methylene protons of —CH_2Cl).

As shown in the ^{1}H-NMR spectrum of PE-F_{13}, the new peaks at 7.02–7.20 ppm were assigned to the hydrogen atoms of substituted benzene (n). The new peaks at 4.43–4.5 ppm were ascribed to the hydrogen atoms of methylene (o). The new proton peaks for —NH—C(O) — (k) were found at 8.61–8.85 ppm. The peaks at 2.6–2.76 ppm were assigned to the hydrogen atoms of methylene (p) connected to —CF_2—. The peaks for the hydrogen atoms of methyl (h) connected to benzene ring were found at 2.11–2.38 ppm. The ^{1}H-NMR spectrum of PE-F_{17} in Figure 1 showed the similar curves as PE-F_{13}. By comparing the integral values of peaks at the 2.6–2.76 ppm (the methylene protons of —CH_2— connected to —CF_2—) and 3.8–4.0 ppm (the methylene protons of —CH_2Cl), it could be found that the degree of modification of PE-F_{13} and PE-F_{17} were 89.1% and 87.8%, respectively. The results from ^{1}H-NMR proved that fluoroalkyl groups had been successfully connected to the end of PE.

The ^{19}F-NMR spectra of PE-F_n were shown in Figure 2. For instance, as for PE-F_{12}, the fluorine resonances of -CF_2- (h) and -CF_2H (a) were found at −122.4 and −139.1 ppm, respectively. The peaks at −122.8, −124.5, and −130.6 ppm were assigned to the —CF_2— (e), —CF_2 (d,c), —CF_2— (b), respectively. The ratio of integral values of peaks h, e, d+c, b, and a is about 1 : 1 : 2 : 1 : 1, which corresponds well to its molecular structure. The peaks of the corresponding fluorine of PE-F_{13} and PE-F_{17} were also shown in ^{19}F-NMR (Figure 2). The results confirmed that the PE-F_n were successfully synthesized.

Fluorine Content in PE-F_n

It is essential to know the accurate fluorine content in PE-F_n with the aim to make accurate adjustment of the fluorine

content in the cured coatings, and thus evaluate the surface aggregation ability of different fluoroalkyl groups in PE-F_n. The fluorine content in PE-F_n was determined by oxygen-flask combustion and fluoride selective electrode.[12] The theoretical fluorine content in PE-F_n was calculated from the recipes by assuming complete conversion of all reactions. The theoretical and measured fluorine content were listed in Table II. As displayed in Table II, the measured fluorine content was a little lower than the theoretical fluorine content, mostly caused by the incomplete conversion of —NCO due to the steric hindrance of —CH_3 in TDI. The degree of modification calculated from fluorine content were almost consistent with those evaluated from ^{1}H-NMR.

Surface Properties of the Cured Coatings

Contact angle of a liquid on a coating surface directly reflects the wettability of the surface. In this study, to examine how structure and concentration of the synthesized fluorinated additive affect the wettability of cured coatings, a series of samples were prepared by adding PE-F_n into the PE powder coating at

Table III. Composition of Powder Formulations

| PE (wt %)	PE-F_n (wt %)	Fluorine content (wt %)
100	0	0
PE + PE-F_{12}		
99.75	0.25	0.016 ± 0.0002
99.50	0.50	0.032 ± 0.0003
99.25	0.75	0.048 ± 0.0005
99.00	1.00	0.064 ± 0.0006
98.50	1.50	0.096 ± 0.0009
98.00	2.00	0.128 ± 0.0012
PE + PE-F_{13}		
99.75	0.25	0.017 ± 0.0002
99.50	0.50	0.035 ± 0.0005
99.25	0.75	0.052 ± 0.0007
99.00	1.00	0.069 ± 0.0009
98.50	1.50	0.104 ± 0.0014
98.00	2.00	0.138 ± 0.0018
PE + PE-F_{17}		
99.75	0.25	0.022 ± 0.0002
99.50	0.50	0.044 ± 0.0004
99.25	0.75	0.065 ± 0.0005
99.00	1.00	0.087 ± 0.0007
98.50	1.50	0.131 ± 0.0010
98.00	2.00	0.175 ± 0.0014
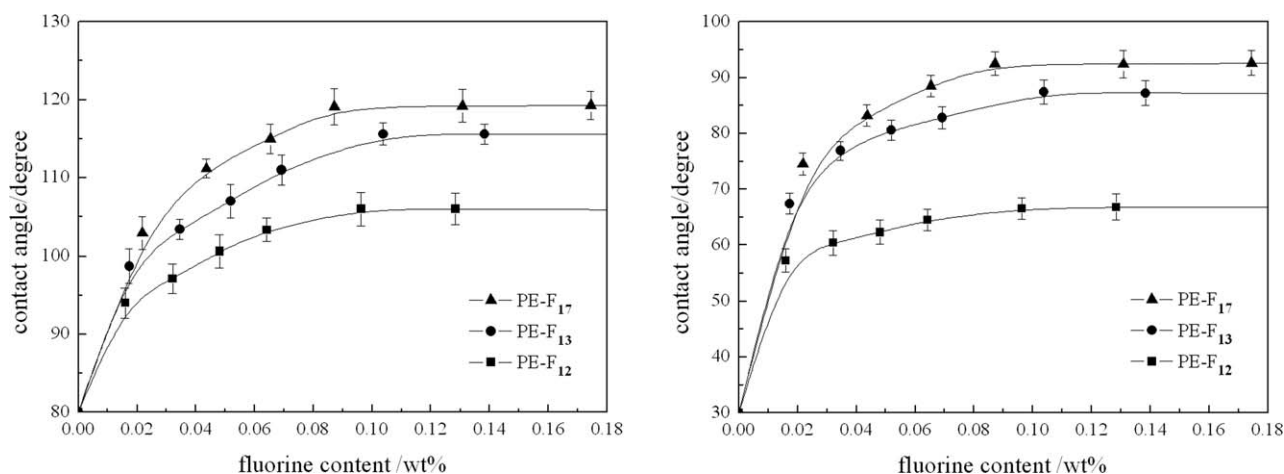
Figure 3. Change of the (a) contact angle of water and (b) diiodomethane on cured coatings with different fluorine content.

the concentration ranging from 0.25% up to 2%, which corresponded to the fluorine content from 0.016 to 0.175% in the PE powder coating (Table III). The fluorine content in the bulk was calculated from the addition concentration of PE-F_n and the measured fluorine content of the PE-F_n itself. The change of the contact angle of water and diiodomethane on cured coatings with different fluorine content was shown in Figure 3.

The contact angle of water and diiodomethane on cured coatings increased with the increase of the fluorine content and then reached the maximum value, indicating that all synthesized fluorinated additives (PE-F_n) enhanced the hydrophobicity and oleophobicity of the cured coatings. For instance, without the addition of PE-F_n, the contact angle of water and diiodomethane on the coating surface were only 80° and 30°, respectively. With the addition of PE-F_{17}, the cured coating became highly hydrophobic and oleophobic with dependence on the fluorine content, and the maximum value of the contact angle of water and diiodomethane reached 119° and 92°, respectively at the fluorine content of 0.087%. Further increase of the concentration of PE-F_{17} made little change on the contact angle of water and diiodomethane, which may be ascribed to the saturation of fluoroalkyl group arrangement on the coating surface. The similar trends with PE-F_{12} and PE-F_{13} were also observed except for lower maximum contact angles both for water and diiodomethane drops. This indicated that the hydrophobicity and oleophobicity of cured coating not only depended on the fluorine content, but also relied on the structure of fluoroalkyl group in PE-F_n. The comparison of contact angle results confirmed that fluoroalkyl groups with —CF_3 at its end had the higher tendency to enrich on the coating surface, which may be ascribed to the lower critical surface tension of —CF_3 (6 mN/m) as compared to —CF_2H (15 mN/m).[18] Moreover, it was also found that the longer perfluoroalkyl groups had the better aggregating ability on the coating surface. This effect may be due to an increase in the segmental mobility of the perfluoroalkyl groups in PE-F_n with an increase in their length.[19]

The surface free energy of cured coatings can be estimated by using geometric mean method [eqs. (1–3)[20,21]] on the basis of contact angles of two liquids.

$$(1+\cos\theta_{H_2O})\gamma_{H_2O}=2\left(\gamma^d_{H_2O}\gamma^d\right)^{\frac{1}{2}}+2\left(\gamma^p_{H_2O}\gamma^p\right)^{\frac{1}{2}} \quad (1)$$

$$(1+\cos\theta_{CH_2I_2})\gamma_{CH_2I_2}=2\left(\gamma^d_{CH_2I_2}\gamma^d\right)^{\frac{1}{2}}+2\left(\gamma^p_{CH_2I_2}\gamma^p\right)^{\frac{1}{2}} \quad (2)$$

$$\gamma=\gamma^d+\gamma^p \quad (3)$$

In which γ was surface free energy, γ^d represented surface free energy of dispersive component, γ^p stood for surface free energy of polar component, θ_{H_2O} and $\theta_{CH_2I_2}$ were contact angles of water and diiodomethane on the cured coatings, respectively. The values of γ_{H_2O}, $\gamma_{CH_2I_2}$, $\gamma^d_{H_2O}$, $\gamma^p_{H_2O}$, $\gamma^d_{CH_2I_2}$, and $\gamma^p_{CH_2I_2}$ were 72.8, 50.8, 22.1, 50.7, 50.4, and 0.4 mJ/m^2, respectively.[22]

The surface free energy of cured coatings was shown in Figure 4. It could be observed that by adding extremely low concentration of PE-F_n, the surface free energy came down sharply from 41.2 to 11.6 mJ m^{-2} (the lowest value). For instance, the surface free energy of cured coatings significantly decreased with the increase of the concentration of PE-F_{17} at first and then remained constant at the concentration of about 1 wt %. The similar trends with PE-F_{12} and PE-F_{13} were observed except for higher minimum surface free energy and the result was consistent with those obtained from the contact angles.

From Figures 3 and 4, it could be concluded that the addition of extremely low concentration of PE-F_n could significantly improve the hydrophobicity and oleophobicity of PE powder coating. Moreover, PE-F_{17} showed the most efficient enhancement at the lowest fluorine content because the PE-F_{17} itself had higher fluorine content than PE-F_{12} or PE-F_{13}, indicating that PE-F_n with longer perfluoroalkyl groups had the higher tendency to aggregate on the coating surface.

Enrichment of Fluoroalkyl Groups on the Coating Surface
It had been shown that the contact angles of water and diiodomethane increased with the addition of low concentration of PE-F_n due to the aggregation of low surface energy components on the coating surface. In this study, XPS analysis was used to determine the chemical composition and surface enrichment of fluoroalkyl groups on the surface of cured coatings.
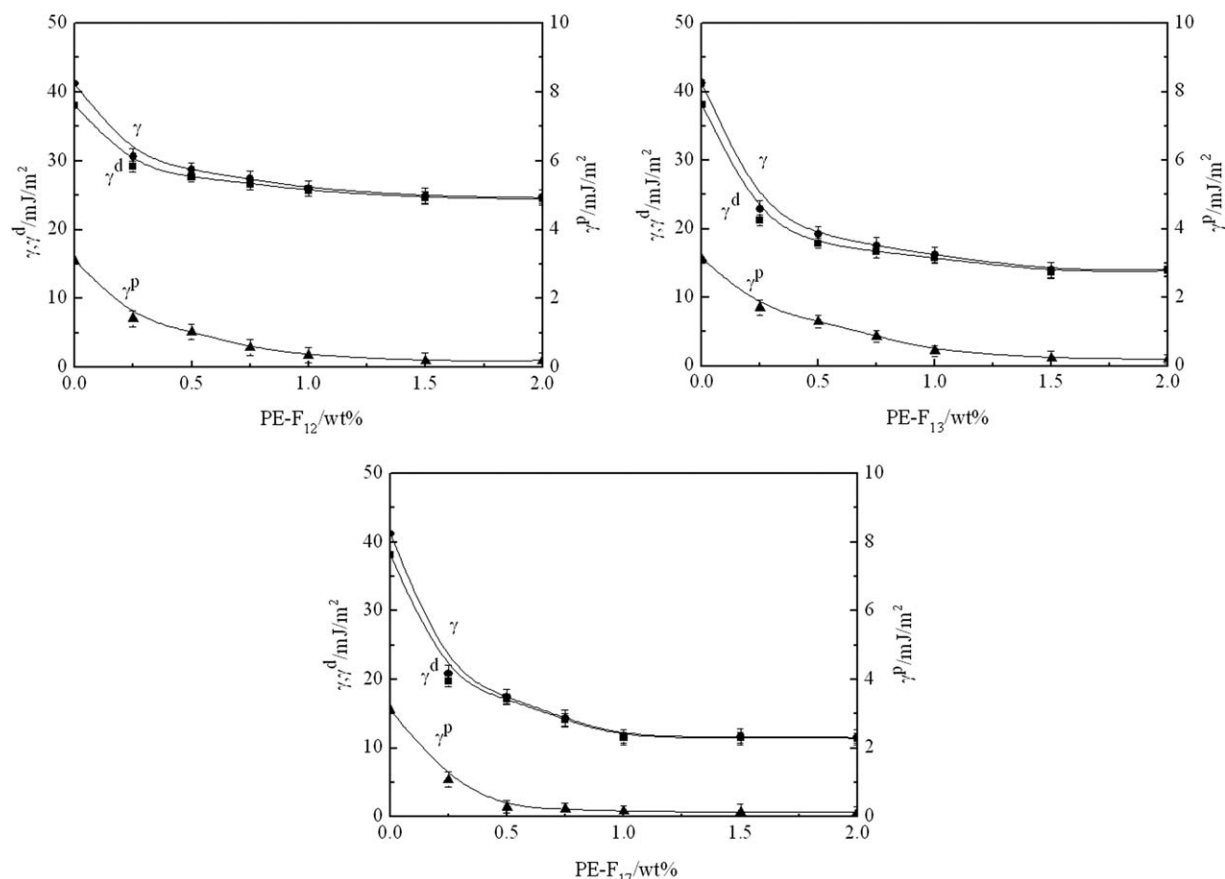
Figure 4. Surface free energy of cured coatings with different concentration of (a) PE-F_{12}, (b) PE-F_{13}, and (c) PE-F_{17}.

The XPS spectra (at the takeoff angle of 15°) of the region corresponding to 0–1000 eV for the cured coatings were shown in Figure 5. In the cured coatings investigated by XPS, PE-F_{12}, PE-F_{13}, and PE-F_{17} were introduced with the concentration of 1.5, 1.5, and 1% (the best concentration of fluorine-containing coating), respectively. It should be noted that the cured coating

containing 1 wt % of PE-F_{17} had the lowest fluorine content in the bulk though the PE-F_{17} itself had the highest fluorine content (Table III). From the survey scan, peaks at 195.1, 284.7, 399.8, 527.3, 598.1, and 684.5 eV were observed and ascribed to Cl_{2p}, C_{1s}, N_{1s}, O_{1s}, F_{KLL}, and F_{1s}, respectively. It could also be observed that the cured coating with addition of PE-F_{17} (the concentration of 1%) showed the highest characteristic peaks of fluorine, suggesting that fluoroalkyl groups in PE-F_{17} had best enrichment effect on the coating surface and the result was consistent with those obtained from the contact angle measurement.
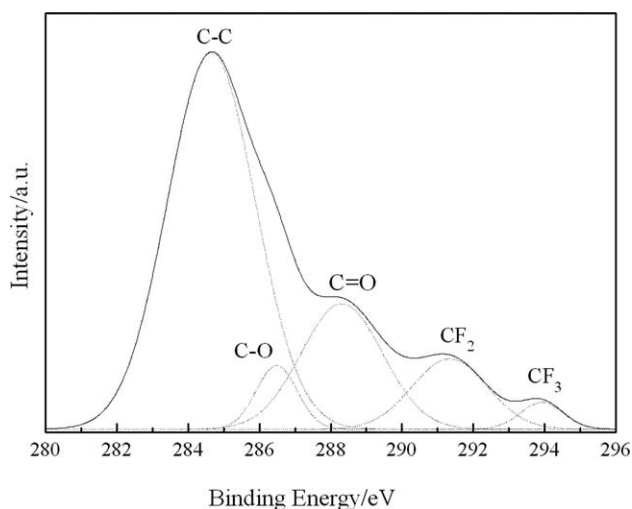

Figure 6. High-resolution C_{1s} XPS spectrum of the cured coating containing 1 wt % PE-F_{17}.
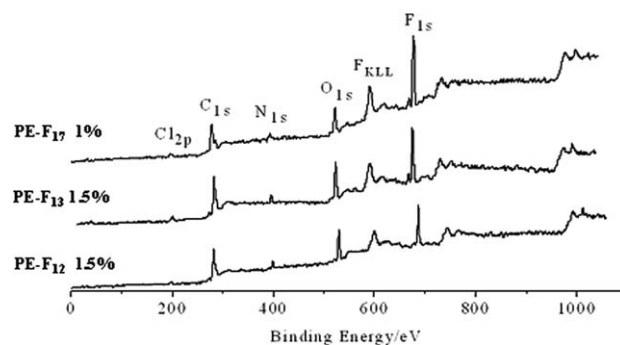

Figure 5. XPS survey scan spectra of the cured coatings with addition of PE-F_n.
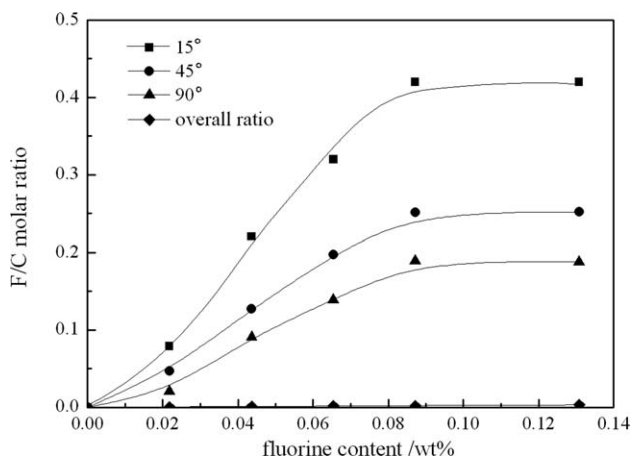
Figure 7. Change of the F/C molar ratio on the coating surface containing PE-F_{17} with the fluorine content (the overall F/C molar ratio was estimated from the recipes by assuming complete conversions of all reactions).

PE-F_{17} was the most effective one in improving the water and oil repellence of cured coatings in the above studies, thus the high resolution spectra of C_{1s} and F_{1s} for the cured coatings with addition of PE-F_{17} were also collected to investigate the

surface enrichment of fluoroalkyl groups on the coating surface. Shown in Figure 6, the curve-fitting analysis of C_{1s} region for the cured coating containing 1 wt % of PE-F_{17} indicated the presence of five kinds of carbon atoms (284.7 eV (aromatic hydrocarbons), 286.4 eV ($-CH_2OC(O)-$), 288.7 eV ($-CH_2OC(O)-$), 291.3 eV ($-CF_2-$), and 293.9 eV ($-CF_3$)).

The F/C molar ratio on the coating surface was calculated according to the high resolution spectra by comparing the F_{1s} and C_{1s} peak intensities [eq. (4)].[16]

$$\frac{n_F}{n_C} = \frac{I_F/S_F}{I_C/S_C} \qquad (4)$$

where I_C and I_F represented the areas of C_{1s} and F_{1s} peaks, respectively. S_C and S_F were the sensitivity factors of C and F (0.296 for C, 1.00 for F), respectively.

In our experiments, in order to investigate the fluorine distributions along film-thickness direction, the takeoff angles of 15°, 45°, and 90° were taken correspond to the detection depths of ∼1.9, 5.2, and 7.3 nm, respectively. Change of the F/C molar ratio on the coating surface containing PE-F_{17} with the fluorine content was presented in Figure 7. The F/C molar ratio on the coating surface increased with the increase of fluorine content and became almost unchanged at the fluorine content of about
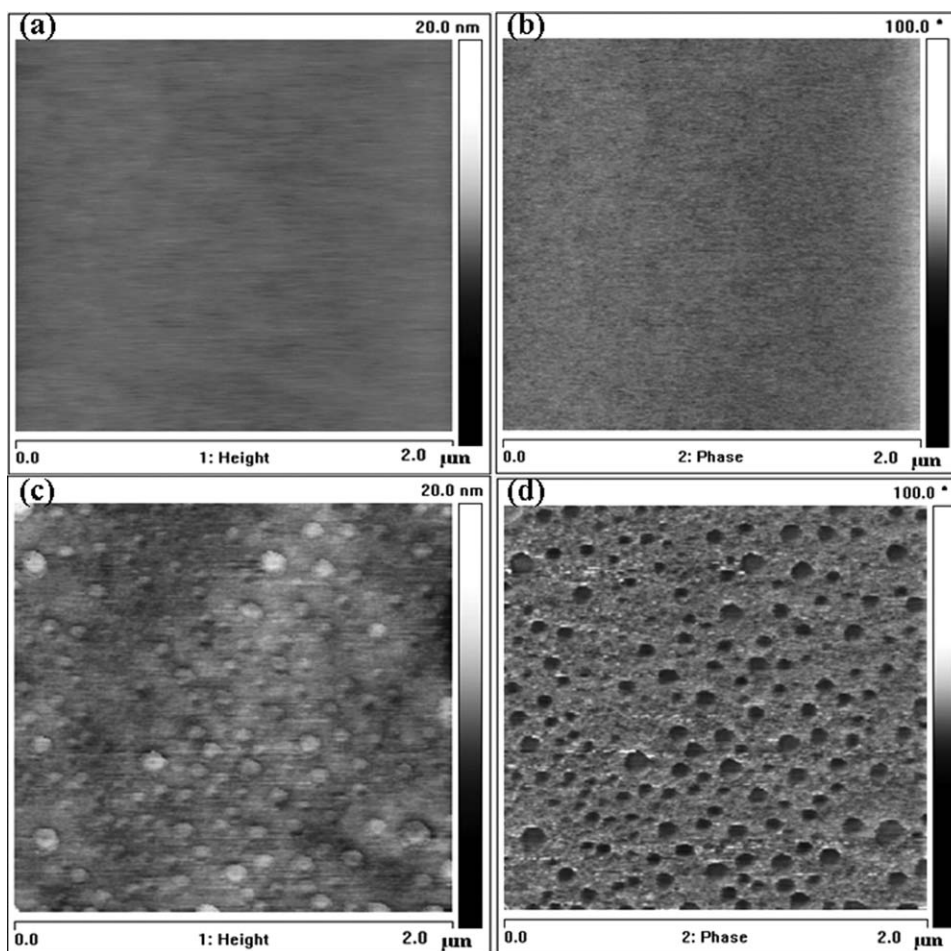

Figure 8. AFM images for fluorine-free cured coating [height (a) and phase (b)] and cured coating with addition of 1 wt % PE-F_{17} [height (c) and phase (d)].

0.087%, which was in agreement with the contact angle data depicted in Figure 3. When the overall F/C atomic ratio was only 0.0025 at the fluorine content of 0.087%, the F/C atomic ratio on the coating surface reached 0.42 at the takeoff angle of 15°, which indicated that the F/C atomic ratio on the coating surface was much higher than the overall F/C molar ratio. It was observed that the F/C atomic ratio at the detection depth of 1.9 nm are higher than those at 5.3 and 7.3 nm, which indicated that the fluoroalkyl groups in PE-F$_{17}$ become more concentrated near the coating surface. Thus, it was confirmed that fluoroalkyl groups were preferentially arranged and concentrated near the coating surface and that a gradient of fluorine existed from surface to the bulk of the cured coatings.

Topological Investigations on Cured Coatings

To study the surface topological structure of cured coatings, AFM measurements under tapping mode were carried out. Figure 8 showed the AFM images of cured coatings (including fluorine-free cured coating and cured coating with addition of 1 wt% PE-F$_{17}$).

AFM height and phase images for the fluorine-free cured coating based on PE were shown in Figure 8(a,b). With scan areas of 2×2 μm^2, the root-mean-square (rms) roughness is around 0.34 nm for height images. It was shown in phase images that the chemical composition was quite uniformly distributed along the coating surface as we expected.

However, the totally different height and phase images were obtained from cured coating with addition of 1 wt % PE-F$_{17}$ [Figure 8(c,d)]. Some domain structure can be easily observed in both height and phase images. The length and the height of the domain of these patterns were about 25–55 nm and 2–3 nm, respectively. It was believed that the dark areas are ascribed to fluoroalkyl species, whereas the light areas correspond to nonfluoroalkyl species according to the former studies.[23] These results suggested that some fluorinated domains were formed on the coating surface. It was therefore evident that there is a preferential enrichment of the fluoroalkyl groups on the coating surface.

CONCLUSION

The PE was successfully modified with fluorinated isocyanate to introduce the fluoroalkyl groups to its ends. The contact angle results showed that the contact angle as additives increased with the increase of fluorine content and then remained constant. An extremely low concentration of PE-F$_n$ in PE powder coating could efficiently decrease the surface free energy and significantly improve the hydrophobicity and oleophobicity of PE powder coating. XPS results showed that the surface F/C molar ratio was much higher than the overall F/C molar ratio due to the fluorine enrichment on the coating surface and a fluorine depleted layer formed beneath the coating surface. The contact angle and XPS results also suggested that longer fluoroalkyl groups and fluoroalkyl groups with —CF$_3$ at its end had the better aggregating ability on the coating surface. Moreover,

AFM results confirmed that the fluoroalkyl groups in PE-F$_n$ had enriched on the coating surface.

REFERENCES

1. Johnson, L. K.; Sade, W. T. *J. Coat. Technol.* **1993**, *65*, 19.

2. Belder, E. G.; Rutten, H. J. J.; Perera, D. Y. *Prog. Org. Coat.* **2001**, *423*, 142.

3. Cerea, M.; Zheng, W. J.; Young, C. R.; McGinity, J. W. *Int. J. Pharm.* **2004**, *279*, 127.

4. Frings, S.; van Nostrum, C. F.; van der Linde, R.; Meinema, H. A.; Rentrop, C. H. A. *J. Coat. Technol.* **2000**, *72*, 83.

5. Su, Y. C.; Chang, F. C. *Polymer* **2003**, *44*, 7989.

6. Van Ravenstein, L.; Ming, W.; van de Grampel, R. D.; van der Linde, R.; de With, G.; Loontjens, T.; Thüne, P. C.; Niemantsverdriet, J. W. *Macromolecules* **2004**, *37*, 408.

7. Pilch-Pitera, B. *J. Appl. Polym. Sci.* **2012**, *124*, 3302.

8. Jin, Y. Q.; Shentu, B. Q.; Weng, Z. X. *J. Appl. Polym. Sci.* **2012**, *125*, 3068.

9. Miao, H.; Cheng, L. L.; Shi, W. F. *Prog. Org. Coat.* **2009**, *25*, 71.

10. Uragmi, T.; Yamada, H.; Miyata. T. *Prog. Org. Coat.* **2006**, *39*, 1890.

11. Miao, H.; Bao, F. F.; Cheng, L. L.; Shi, W. F. *J. Fluorine Chem.* **2010**, *131*, 1356.

12. Geng, W. H.; Nakajima, T.; Takanashi, H.; Ohki, A. *Fuel* **2008**, *87*, 715.

13. Jin, Y. Q.; Shentu, B. Q.; Weng, Z. X. *Chem. React. Eng. Technol.* **2011**, *27*, 353.

14. Jin, F. Y.; Jin, X. H. *Chem. Anal.* **2004**, *40*, 237.

15. Liu, H. J.; Lin, L. H.; Chen, K. M. *J. Appl. Polym. Sci.* **2003**, *88*, 1236.

16. Briggs, D. Surface Analysis of Polymers by XPS and Static SIMS; Cambridge University Press: Cambridge, **1998**; Chapter 2.

17. Bartelink, C. F.; de Pooter, M.; Grunbauer, H. J. M.; Beginn, U.; Moller, M. *J. Polym. Sci. A: Polym. Chem.* **2000**, *38*, 2555.

18. Shafrin, E. G.; Zisman, W. A. *J. Phys. Chem.* **1960**, *64*, 519.

19. Korolev, L. V.; Kuzina, N. G.; Mashlyakovskii, L. N. *Russ. J. Appl. Chem.* **2011**, *84*, 12462.

20. Heitz, J.; Dickinson, J. T. *Appl. Phys. A Mater. Sci. Process.* **1999**, *68*, 515.

21. Li, K.; Wu, P. P.; Han, Z. W. *Polymer* **2002**, *43*, 4079.

22. Shimizu, R. N.; Demarquette, N. R. *J. Appl. Polym. Sci.* **2000**, *76*, 1831.

23. Sauer, B. B.; Mclean, R. S.; Thomas, R. R. *Langmuir* **1998**, *14*, 3045.